

---

# The Half Million Quasars (HMQ) Catalogue

---

Eric W. Flesch

PO Box 5, Whakatane, New Zealand  
Email: [eric@flesch.org](mailto:eric@flesch.org)

(RECEIVED December 10, 2014; ACCEPTED February 20, 2015)

## Abstract

A quasar catalogue is presented with a total of 510 764 objects including 424 748 type 1 QSOs and 26 623 type 1 AGN complete from the literature to 2015 January 25. Also included are 25015 high-confidence SDSS-based photometric quasars with radio/X-ray associations, 1595 BL Lac objects, and 32783 type 2 objects. Each object is displayed with arcsecond-accurate astrometry, red and blue photometry, redshift, citations, and radio and X-ray associations where present. Also, 114 new spectroscopically confirmed quasars are presented.

Keywords: catalogues – quasars: general

## 1 INTRODUCTION

We have entered an era of large data where accuracy and completeness are the expected norm in every data-driven endeavour. If the project includes legacy data, however, then particular challenges are faced to bring that legacy data up to today's standard. So it is with quasar cataloguing which includes 20th century legacy data having paper-specific astrometry and photometry standards of great variance. These were catalogued as reported, most recently in the Véron-Cetty & Véron Catalogue of Quasars and Active Nuclei 13th edition (VCV: Véron-Cetty & Véron 2010), although the Vérons worked to improve data quality throughout their releases with good success; in their last five releases I contributed a small assist by auditing their pre-release data to find any anomalies. However, arcsecond-accurate astrometry was not achieved for some thousands of objects and classifications were unreliable for 3% of objects as will be detailed below. Thus the legacy quasar data needed to be cleaned to today's standard to integrate that data into the databases of today.

This paper presents a new quasar catalogue which is complete from the literature to 2015 January 25, bears arcsecond-accurate astrometry and uses a higher threshold to accept objects as quasars. This 'Half Million Quasars' (HMQ) catalogue was extracted from the on-line unpublished 'Milliquas'<sup>1</sup> catalogue which includes photometric and radio/X-ray associated quasar candidates. Over the past few years I have worked to resolve all issues remaining in the legacy data to where I can now present 100% reliable astrom-

etry and 99% reliable classifications for all objects. Resolved issues are discussed below and outcomes tabulated.

The HMQ catalogue presents a complete survey of type 1 QSOs/AGN from the literature; type 2 objects are included as a convenience to the user but only at  $\approx 90\%$  completeness from the literature because they are such a heterogeneous group from many criteria used throughout 50 years of discovery; nowadays type 2 is used in a practical way to show narrower emission lines than type 1. This catalogue signals a shift from the VCV philosophy of including questionable objects (so flagged by their discoverers) as quasars, so such objects are dropped. BL Lac objects are included to continue VCV's tradition of including them. Also some high-confidence photometric quasar candidates with radio/X-ray associations are included as discussed in [Section 8](#).

The intent here was to present original quasar names and best redshifts. VCV usually presented original names but sometimes they substituted other forms based on astrometry or unclear provenance; I recovered some original names along the way. The SDSS<sup>2</sup> re-surveyed many legacy objects without always acknowledging the original identifications, but those original identifications are reported here. Part of the problem would have been the discrepant early astrometry but that is now fully resolved. SDSS redshifts are preferred and usually substituted for original discovery redshifts, and so cited.

Accordingly, the catalogue presented here brings the community's quasar archive to a high standard of usability where each quasar is recorded with arcsecond-accurate astrometry (out to 2 arcsec for some legacy objects), its original name

---

<sup>1</sup>Milliquas: <http://quasars.org/milliquas.htm>, also on NASA HEASARC at <https://heasarc.gsfc.nasa.gov/W3Browse/all/milliquas.html>

<sup>2</sup>Sloan Digital Sky Survey, <http://sdss.org>

**Table 1.** Sample lines from the HMQ.

RA (J2000)	DECL	NAME	TYPE	RMAG	BMAG	COM	PSF	Z	REF	ZREF	X-RAY	CORE RADIO	LOBE or EXTRA 1	LOBE or EXTRA 2	
185.3765271	28.0982751	SDSS J122130.36+280553.7	qX	20.6	20.7	g	--	2.100	225	1537	XMMX J122130.3+280553		1WGA J1221.5+2805	15XP5 J122130.2+280553	
185.3766440	-2.6924870	2QZ J122130.3-024134	QR2	19.4	20.1	p	--	1.277	447	1668		FIRST J122130.4-024132	FIRST J122131.4-024133	FIRST J122129.4-024135	
185.3769821	12.2726142	SDSS J122130.47+121621.4	Q	20.2	20.9	j+m	-1	2.504	1409	1410					
185.3771700	15.3422690	SDSS J122130.52+152032.1	AR	21.8	22.9	g	1	1	0.705	28	34	FIRST J122130.5+152032	NVSS J122130.5+152033		
185.3777010	-0.4519630	ZSLAQ J122130.65-002707.1	Q	21.6	21.6	g	--	1.807	448	448					
185.3783740	14.6949813	SDSS J122130.80+144141.9	QX	20.6	20.8	g	--	2.673	1409	1410	3XMM J122130.8+144142				
185.3786112	-6.9497223	HE 1218-0640	Q	16.3	16.6	p	--	1.403	2085	2085					
185.3790680	1.1244030	2QZ J122130.9+010727	Q	17.5	17.7	p	--	1.370	447	1668					
185.3791722	29.9063436	SDSS J122131.00+295422.8	QX	20.1	20.3	p	--	2.592	1410	1410	3XMM J122131.0+295425				
185.3791879	54.3750213	SDSS J122131.00+542230.0	Q	19.9	20.6	j	-1	3.515	1410	1410					
185.3796250	-13.9004444	PKS 1218-136	ARX	14.8	17.1	p+	1	1	0.103	1224	1224	15XP5 J122131.0-135404	NVSS J122131.1-135402		
185.3801250	-2.0247744	2QZ J122131.2-020130	Q	19.6	21.1	p	--	1.613	447	447					
185.3805535	11.0905695	SDSS J122131.33+110526.0	Q	19.8	21.0	j	--	4.118	1666	1410					
185.3806810	44.4663940	SDSS J122131.36+442759.0	QR	18.7	19.1	g	--	1.530	1667	1668		FIRST J122131.3+442759			
185.3810198	44.3690126	SDSS J122131.44+442208.4	Q	18.3	21.4	j	-1	3.237	1410	1410					
185.3813933	10.1076430	SDSS J122131.53+100627.5	Q	19.0	19.8	p	--	1.967	1666	1410					
185.3819287	-1.3565540	2QZ J122131.6-012124	Q	20.3	20.7	j	1	-1.870	447	447					
185.3820628	28.2328960	ON 231	BRX	13.9	15.3	p	1	1	0.103	261	11	15XP5 J122131.7+281357	FIRST J122131.6+281358	NVSS J122131.6+281358	XMMX J122131.7+281359
185.3832097	45.3013942	SDSS J122131.97+451805.0	Q	21.4	21.7	g	--	0.953	1410	1410					
185.3836112	8.3622794	RXJ J12215+0821	KRX	19.2	18.6	p	n	n	0.132	139	29	1RXS J122131.4+082139	FIRST J122132.0+082144	NVSS J122132.0+082143	
185.3844156	32.5256413	SDSS J122132.25+323132.3	Q	21.6	21.5	g	--	2.639	1408	1410					
185.3848150	30.3337552	SDSS J122132.35+302001.5	QX	21.7	21.6	g	--	2.327	1410	1410	3XMM J122132.2+302003				
185.3850658	4.5993659	SDSS J122132.41+043557.7	qRX	20.7	20.8	g	--	2.100	225	1537	CX0 J122132.4+043558	FIRST J122132.4+043557	NVSS J122132.1+043558	3XMM J122132.4+043557	

Notes on columns (see ReadMe for full descriptions):

- TYPE: 1st char is the object classification: Q=QSO, A=AGN, B=BL Lac type, q=photometric, K=type 2; see Section 5. Extra chars summarise the associations displayed: R=radio, X=X-ray, 2=double radio lobes.
- COM: comment on photometry: p=POSS-I magnitudes, so blue is POSS-I O, j=SERC Bj, g=SDSS green, +=optically variable, m=nominal proper motion.
- PSF: for red and blue sources: ‘-’=stellar, 1=fuzzy, n=no psf available, x=not seen in this colour.
- REF & ZREF: citations for name and redshift; citations are indexed in the file ‘HMQ-references.txt’.
- LOBE or EXTRA: if TYPE shows a ‘2’ (=lobes), then double radio lobe identifiers are displayed here. Otherwise, any additional radio and/or X-ray identifiers are displayed here.

The full table can be downloaded from <http://quasars.org/HMQ.htm>, also available in FITS.

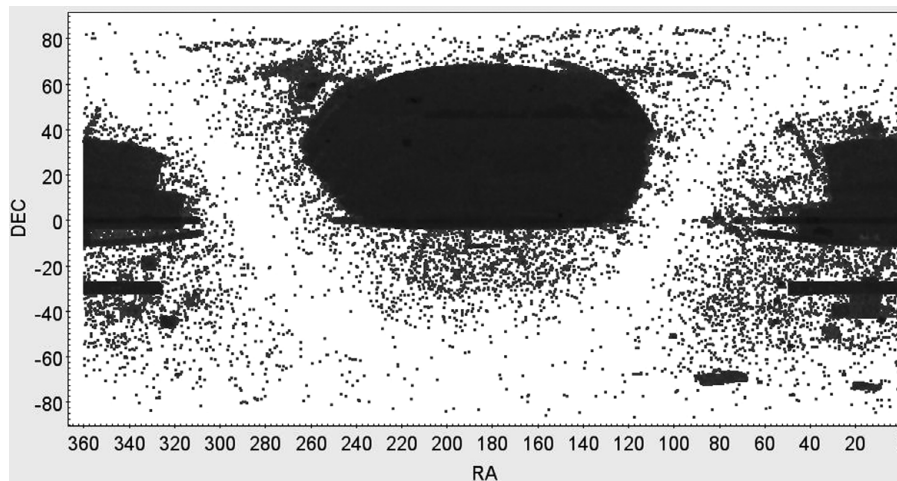


**Figure 1.** Sky coverage of the HMQ.

and discovery citation, red and blue photometry, best redshift with citation, and radio/X-ray associations. The catalogue is available in both flat file and FITS formats<sup>3</sup> and has a ReadMe which describes the contents and source data therein. Table 1 shows a few sample lines of the flat file with some explanation of the columns, but the HMQ ReadMe gives full details of the layout and contents. Figure 1 shows the sky coverage of the HMQ; the high density blocks of coverage are primarily from the SDSS; the high density strip at decl  $-30^\circ$  is from the 2dF QSO Redshift Survey (2QZ: Croom et al. 2004).

The sections below describe the issues involved in constructing this catalogue, including data acquisition from the legacy VCV catalogue and the SDSS catalogues which sup-

ply most quasars, quasars newly published here, and the inclusion of high-confidence photometric quasars. AGN classification is detailed. Photometry and radio/X-ray associations are summarised with references given.

## 2 THE VCV OPTICAL CATALOGUE

A fundamental part of constructing the HMQ was to audit and incorporate the best previous comprehensive catalogue of quasars, which is of course the Véron-Cetty & Véron Catalogue of Quasars and Active Nuclei 13th edition (Véron-Cetty & Véron 2010). However, VCV included astrometry and identifications which were not always optically based, for legacy reasons. In Flesch (2013), I promulgated the need to convert that to a fully optical presentation to enable easy

<sup>3</sup>at <http://quasars.org/HMQ.htm>

inclusion into dynamic databases like NED<sup>4</sup> and SIMBAD<sup>5</sup>, and in service of that I presented the true position or status of 449 VCV objects which hitherto had no obvious optical counterpart. I have continued that task to where the VCV catalogue is now fully mapped, line for line, into the optical J2000. This ‘VCV Optical catalogue’<sup>6</sup> identifies and resolves all anomalies including those reported in Flesch (2013). Following is a summary of those issues, and lists of objects supplementary to those presented in Flesch (2013).

VCV presented 167 567 QSOs/AGN of which 160 271 were subclassed as type 1 (or had no subclass), 6 203 as type 2, 926 as LINER galaxies, and 167 as starburst galaxies; also 1 374 BL Lac objects were listed, thus 168 941 in total. The HMQ optical mapping, with the benefit of SDSS data through DR12, resolves these as 156 322 type 1, 1 142 BL Lac objects, 4 662 type 2, 747 LINERs, 5 024 galaxies, 267 stars, 667 objects of unknown classification (usually from SDSS-DR7 or later SDSS releases which dropped them), 8 satellite streaks, 2 asteroids (i.e., 3-colour strobes on SDSS), 2 star spikes, 61 duplicates of other VCV objects, and 37 objects which are lost or never existed. It behoves me to explain these reclassifications, so first I list out the most involved discovery papers (the individual objects involved are listed in the VCV Optical catalogue with these citations):

(A) 4 113 objects were re-classified as stars or non-AGN galaxies by papers subsequent to VCV, usually SDSS releases:

1. 3 424 by SDSS-DR8 Aihara et al. (2011) due to re-processing of the spectra via an improved algorithm.
2. 291 by SDSS-DR12Q Pâris et al. (2015) which reclassified many objects via visual inspection of the spectra.
3. 267 by SDSS-DR9Q Pâris et al. (2012) which reclassified many objects via visual inspection of the spectra.
4. 42 by SDSS-DR10Q Pâris et al. (2014) which reclassified many objects via visual inspection of the spectra.
5. 39 by SDSS-DR9 Ahn et al. (2012) via an improved automated pipeline.
6. 25 by SDSS-DR10 Ahn et al. (2014) via an improved automated pipeline.
7. 14 by Kleinman et al. (2013) which identified white dwarfs from the SDSS-DR7 data.
8. 5 by Ge et al. (2012) which identified double-peaked narrow emission line galaxies (NELGs).
9. 6 other objects from 4 papers.

(B) 1 845 objects were originally classified as stars or non-AGN galaxies by their discovery papers but taken up by

VCV as ‘active galaxies’, or were reclassified as non-AGN prior to VCV’s final edition but VCV retained the original classification:

1. 473 from Schneider, Schmidt, & Gunn (1994) which classified these as emission-line galaxies (ELGs) of  $z < 0.45$ .
2. 430 from SDSS-DR7 Abazajian et al. (2009) which classified these as stars or non-AGN galaxies, confirmed by their exclusion from SDSS-DR7Q Schneider et al. (2010). Many of these had been classified as AGN by earlier publications.
3. 261 from the 2dF Galaxy Redshift Survey (2dFGRS: Colless et al. 2001) which is a large galaxy catalogue without QSO classifications. VCV extracted high-redshift objects and others with emission lines showing activity, but visual inspection of the high-redshift objects reveal that they are often confused with closely co-positioned neighbours. Some of these objects were cited elsewhere and included by VCV on that basis, but subsequent SDSS classifications are as galaxies only. The optical appearance of almost all of these objects is that of galaxies, and only 16 show radio/X-ray association. I see no avenue by which to retain these objects as type I AGN, so they are dropped.
4. 144 from Iovino, Clowes, & Shaver (1996) were annotated by them with ‘?’ signifying spectral overlap or possible star. Many of these are anomalously bright and none show radio/X-ray association, so they are all dropped. Some of the remaining 1 140 objects from that paper are quite bright or reddish, so caution in their use is indicated.
5. 88 from the 2QZ Croom et al. (2004), which classified 85 of these as ‘continuum’ objects and 3 as NELGs. None show radio/X-ray association and all of the continuum objects were marked by VCV as ‘BL?’ showing that they were questionable, so they are dropped.
6. 64 from Mauch & Sadler (2007) who classified these as LINERs.
7. 47 from Schneider, Schmidt, & Gunn et al. (1999) who, as with their 1994 paper, classified these as ELGs of  $z < 0.45$ .
8. 45 from La Franca et al. (1999) which classified these as ELGs.
9. 25 from Barcons et al. (2007) which classified these as NELGs.
10. 18 from Sandage & Bedke (1994) which classified these NGC galaxies as LINERs and starburst.
11. 10 from Gaston (1983a) and 2 from Gaston (1983b), both of which surveyed SA57 (i.e., ‘selected area 57’), but these 12 are without quasar colours or radio/X-ray association. Gaston (1983b), sec III, qualified that the SA57 photometry had ‘much greater scatter’ and ‘nonuniformity’

<sup>4</sup>NASA/IPAC Extragalactic Database, <http://ned.ipac.caltech.edu>

<sup>5</sup>SIMBAD database at CDS, <http://simbad.u-strasbg.fr/simbad>

<sup>6</sup>the VCV Optical catalogue is downloadable, with a ReadMe, from <http://quasars.org/HMQ.htm>

**Table 2.** 21 more duplicates in VCV13.

#	VCV Duplicate				Offset arcsec	VCV Master				HMQ			
	Name	tbl <sup>a</sup>	z	Vmag		Name	tbl <sup>a</sup>	z	Vmag	Name	z	Rmag	Bmag
1	IGR J00256+6821	3	0.012		665 E/W	IRAS 00227+6805	3	0.012		ZOAG 120.54+5.61	0.012	13.5	18.3
2	Q 0235+164	3	0.524	20.9	2	AO 0235+164	1	0.940	15.5	Q 0235+164	0.940	18.8	20.2
3	Q 03020-0014	1	3.050	21.5	26	SDSS J03045-0002	1	3.061	20.5	Q 03020-0014	3.060	20.3	20.5
4	1WGA J0827.6+0942	1	0.260	15.5	14	SDSS J08276+0942	3	0.260	18.8	SDSS J082739.00+094209.4	0.260	17.3	18.7
5	JGR J09253+6929	3	0.039		63	IGR J09253+6929	3	0.039		IGR J09253+6929	0.039	13.4	15.2
6	RX J09278+3431	1	0.425	17.8	37 E/W	SDSS J09278+3431	3	0.426	19.5	SDSS J092751.11+343103.6	0.426	17.8	18.1
7	1WGA J0958.0+4903	3	0.234	18.7	14	SDSS J09580+4903	3	0.242	19.0	1WGA J0958.0+4903	0.242	17.5	18.2
8	RX J10514+3358	3	0.183	18.3	48	SDSS J10514+3358	3	0.183	19.4	SDSS J105128.41+335850.8	0.183	17.1	19.0
9	LH 28B	3	0.205	18.8	734 E/W	RX J10543+5725	3	0.205	18.2	RX J10543+5725	0.205	18.4	21.3
10	FIRST J10544+2534	1	2.400	17.5	120 N/S	SDSS J10544+2536	1	1.774	18.4	FBQS J105427.1+253600	2.400	17.5	18.8
11	SBS 1059+599	1	1.830	17.6	47	TEX 1059+599	1	1.830	17.1	TEX 1059+599	1.830	16.9	17.5
12	WEE 43	1	3.009	19.8	21	SDSS J11161+1358	1	3.034	20.0	WEE 43	3.033	19.4	20.9
13	RXS J11479+2715	3	0.364	19.6	60 E/W	US 2964	1	0.363	16.1	US 2964	0.363	16.3	16.4
14	Q 1207+106	1	2.330		150 E/W	SDSS J12098+1021	1	2.312	19.4	Q 1207+106	2.313	19.3	19.8
15	SDSS J13523+1302	1	1.600	18.1	0	H 1400#16A	1	1.600	18.1	H 1400#16A	1.600	17.7	18.0
16	3C 295.0	3	0.461	19.8	60 N/S	SDSS J14113+5212	3	0.462	20.8	3C 295.0	0.461	18.0	20.8
17	RXS J15244+3032	1	0.282	17.2	6	SDSS J15244+3032	1	0.274	16.9	SDSS J152428.67+303237.5	0.274	16.6	16.7
18	Q 1532+01/2	1	0.310	17.5	90 E/W	XBS J15349+0130	3	0.310	18.8	SDSS J153456.20+013032.3	0.308	17.2	18.4
19	ESO 136-G06	3	0.015	14.8	43 056	ESO 136-G006	3	0.015	14.8	ESO 136-6	0.015	13.4	
20	ESO 407-IG17	3	0.091	17.4	16	NVSS J23243-3426	3	0.091	16.1	ESO 407-17	0.091	14.5	14.9
21	CXOMP J23485+0053	1	0.769	20.0	19	CXO J23485+0058	3	0.948	21.3	CXO J23485+0058	0.948	18.8	19.3

<sup>a</sup>VCV Table 1 listed QSOs, Table 3 listed AGN.

compared with concomitant CFHT and KPNO photometry, and in sec II*ai* stated a forthcoming paper, ‘Hoag et al. 1983’, of these SA57 quasars which however never appeared. Edwards, Beauchemin, & Borra (1988) resurveyed SA57, confirming no Gaston object, and related that Hoag in fact ‘did not confirm many of the Gaston candidates’.

- 238 other objects from 117 papers, usually from VCV’s own annotations that they are questionable, or starburst galaxies, etc.

A total of 61 duplications are found in VCV, of which 39 were presented in Flesch (2013) and one in Cupani et al. (2011). The remaining 21 newly-found duplications are listed in Table 2 which displays the VCV names of the wrongly-sited duplicate and correctly-sited master, the offset between them in arcseconds, and the final HMQ name which is usually the original form. One of these, #10 on the list, deserves a special mention in that VCV took the redshift of the master from SDSS-DR6, but that redshift was corrected by SDSS-DR7 to that given by the original discoverers.

As a further supplement to Flesch (2013), Table 3 lists 31 more moves of 30+ arcsec for VCV objects. 29 of these are newly presented, whilst two, #s 4 and 5, are moved from the position given in Flesch (2013) due to better information. Also, four objects were wrongly moved in Flesch (2013), being Q 0004-019, IRAS 12202+1646, and MS 22225+2114 which are returned to their VCV location, and IXO 32 which is moved to its finding chart location at 09 10 20.2 +07 05 55

(J2000). The right-hand column is a comment on the move, ‘OA’=original author.

Also, Flesch (2013) identified 30 VCV objects to de-list because they either are not quasars or have information of such poor quality that the object is lost beyond any mechanism of recovery. In a similar vein, I present 14 VCV objects in Table 4 which are not seen at all, and the methods of Flesch (2013) find no candidate. These objects are obviously not included in the HMQ catalogue.

HMQ has sourced much data directly from large source catalogues like SDSS, 2QZ Croom et al. (2004), etc., so the actual uptake from VCV consists of a residue from smaller papers which amount to 19 127 type 1 objects, 1 083 BL Lac objects, and 1 594 type 2 objects for a total of 21 794 legacy objects. Most of the citations for these legacy objects have been copied from the VCV citation list.

### 3 INCLUSION OF SDSS QUASARS

The majority of quasars in this catalogue are, of course, sourced from the ongoing SDSS releases which have dwarfed in size and complexity all previous quasar surveys; a full description of the SDSS project is beyond the scope of this paper, so the reader is assumed to have some acquaintance with it. There are two simplifications in the HMQ citations: the SDSS data releases 1 and 2 are subsumed into the DR3 release, consistent with their presentation in the SDSS data archives, and DR11 which was an internal release only is similarly subsumed into DR12 and so not considered further.

**Table 3.** 31 more moves of 30+ arcsec in VCV13.

#	VCV					HMQ		
	Name	J2000	tbl <sup>a</sup>	z	Move asec	Name	J2000	Comment
1	ChOPS J04206+3245	042348.6+324522	3	0.307	2271	ChOPS J04206+3245	042048.6+324522	offset 3 time minutes E/W, VCV error
2	ESO 374-G25	100323.6-373339	3	0.023	594	ESO 374-25	100323.7-372345	offset 10 arcmin N/S
3	Q 1257+2843	125951.2+282730	1	2.990	589	Q 1257+2843	125951.1+281741	offset 10 arcmin N/S, OA error
4	Q 0112-27	011452.8-271409	1	2.894	343	Q 0112-27	011517.2-271223	correct position courtesy of Cyril Hazard
5	Q 0752+617	075622.4+613401	1	1.892	234	Q 0752+617	075646.6+613639	optical fit like co-published Q 0932+501
6	RX J08087+0018	080847.1+001801	3	0.019	124	UGC 4248	080855.4+001806	corrected to galaxy position
7	MCG -03.27.026	104217.6-174018	3	0.021	85	MCG -3-27-026	104218.9-173855	corrected to galaxy position
8	F 265	065617.3-653348	3	0.029	78	FAIRALL 265	065629.8-653338	corrected to galaxy position
9	EXO 1429.9+3717	143158.6+370402	1	1.925	74	EXO 1429.9+3717	143201.7+370258	within OA error circle, NBCKDE J143201.72+370257.8
10	F 917	205255.5-515246	3	0.053	64	ESO 235-10	205259.5-515154	corrected to galaxy position
11	G 2344-3852	234649.2-383520	3	0.041	63	PGC 2817464	234643.8-383521	offset 1 arcmin E/W
12	ESO 353-G09	013150.4-330809	3	0.017	59	ESO 353-9	013150.4-330710	offset 1 arcmin N/S
13	Q 1409+732	140949.9+725941	1	3.560	58	Q 1409+732	141003.2+725939	FC was onto plate flaw, 1 arcmin E/W
14	ESO 338-G17	193813.1-385425	3	0.019	58	ESO 338-17	193816.4-385342	corrected to galaxy position
15	MCG -03.04.046	011925.0-154107	3	0.051	53	MCG -3-04-046	011925.0-154200	offset N/S
16	MCG -01.02.013	002600.0-025507	3	0.068	51	MCG -1-02-013	002600.0-025558	offset 50 arcsec N/S
17	MCG -03.02.027	003818.4-145007	3	0.037	49	MCG -3-02-027	003818.4-145056	offset 50 arcsec N/S
18	Q 0139-371	014158.1-365251	1	0.365	48	Q 0139-371	014201.8-365310	finding chart of spectra, OA
19	MCG -01.25.049	095056.5-045906	3	0.022	47	MCG -1-25-049	095056.4-045953	offset 45 arcsec N/S
20	MCG -01.40.001	153318.9-084125	3	0.023	45	MCG -1-40-001	153320.6-084203	corrected to galaxy position
21	F 239	044851.2-573937	3	0.023	43	ESO 119-8	044856.6-573935	corrected to galaxy position
22	MCG -01.30.005	113423.3-094006	3	0.021	42	NGC 3722	113423.2-094048	corrected to galaxy position
23	MCG -02.27.009	103527.3-140707	3	0.015	41	MCG -2-27-009	103527.3-140748	offset 40 arcsec N/S
24	ESO 104-041	190933.3-622839	3	0.085	41	ESO 104-41	190938.8-622855	E gal is AGN, XMMSL J190938.8-622855
25	MCG -02.08.039	030028.2-112504	3	0.030	37	MCG -2-08-039	030030.6-112456	corrected to galaxy position
26	G J0639-5125	063936.8-512515	3	0.108	37	DENISP_G_J0639411-512515	063940.7-512515	offset 4 timesec E/W
27	Q 21570-302	215959.3-300027	1	1.900	36	Q 21570-302	215956.6-300027	35 arcsec offset E/W
28	MCG -02.11.014	040427.5-101006	3	0.031	35	MCG -2-11-014	040427.5-101041	moved 35 arcsec S
29	F 296	022504.3-631320	3	0.057	32	F 296	022509.0-631327	moved 5 timesec E
30	2E 1416+2523	141858.1+251020	1	0.674	32	2E 1416+2523	141857.6+250949	OA specified wrong object, SDSS-DR10 re-found.
31	Q 1606.5+29.1	160831.1+290231	3	0.060	32	KP 1606.5+29.1	160831.6+290200	OA finding chart

<sup>a</sup>VCV Table 1 listed QSOs, Table 3 listed AGN.

**Table 4.** 14 more objects to delete from VCV13.

#	Name	J2000	tbl <sup>a</sup>	mag <sup>b</sup>	z	Comment
1	Q J02397-0135	023947.5-013512	1		1.605	not seen
2	XMM 551B	031243.0-551157	1		0.789	not seen
3	RXS J04014-0801	040126.3-080200	1	14.6	0.147	not seen at $v=14.6$ , OA says "QSO?" questionable
4	Q 0537-44 A1	053850.6-440508	3	21.0	0.885	unseen binary, OA states unclear
5	1H 0828-706	082817.2-704859	1		16.7	approx position, no candidate seen
6	RXS J09052-3350	090517.9-335016	3	20.5	0.425	not seen, OA says NELG
7	COSM J09591+0228	095907.7+022816	1	18.6	0.800	not seen
8	2QZ J095926+0115B	095926.0+011546	1	20.3	1.404	not seen, OA presents no double
9	EXO 1145.1+0031	114741.2+001455	3	19.2	0.096	not seen
10	Q J13053+2902	130520.1+290247	3	20.2	0.076	multiple candidates, unclear if any is QSO
11	Q J13061+2850	130609.1+285028	3	22.1	0.079	not seen
12	SDSS J14111+4249	141107.0+424936	1		1.075	SDSS shows nothing there
13	284_4709	141630.7+520407	3	19.8	0.450	nothing seen
14	RXS J21527+1341	215242.4+134150	1	16.2	0.202	cluster, unclear, OA does not state QSO

<sup>a</sup>VCV Table 1 listed QSOs, Table 3 listed AGN.

<sup>b</sup>Vmag from VCV, can be blank.

In use of the SDSS, it is not enough to simply take up all SDSS ‘quasars’ because they are not as uniformly reliable as that. The SDSS project uses an automated pipeline which matches spectra to standard templates by which any spectrum well-matched to a quasar template is securely classified as a quasar. But of course many spectra are ambiguous fits to templates, especially for faint objects with noisy spectra. To cater for this, the SDSS consortium periodically issues manually-checked quasar catalogues which are much more reliable than the automated ones, the most recent being SDSS-DR12Q Pâris et al. (2015). I use those manual catalogues as a definitive source although they do have a few false objects to remove—indeed, each edition typically drops some objects from previous editions. Objects not accepted into those manual catalogues (i.e., ‘pipeline-only’ objects) may not be quasars or their spectra could be too low quality (i.e., ‘low significance’) to be credible, but often they simply fell on the wrong side of threshold cutoffs such as magnitude or luminosity. Inspection of the spectra of such pipeline-only quasars shows that indeed many are plainly recognisable as quasar spectra, and many are not. Therefore, I needed to find criteria to bulk-separate the high significance pipeline-only quasars from the low, in order to accept the good ones into this comprehensive catalogue. Fortunately this could be done as follows.

As a background, the SDSS data releases 1 to 7 comprise the ‘legacy’ period in which the classifications of quasars, galaxies, stars, and ‘unknowns’ were released as separate incremental tables, and the manual catalogues were quasars only. There was no means of bulk-grading the pipeline-only quasars in the legacy data. The current ‘SDSS3’ data releases 8 to 12 are made as single tables which include all classifications and historical data, and the manual catalogues include a ‘superset’ of all manually inspected classifications. Key enhancements of the SDSS3 releases are the provision of a ZWARNING field which flags problems with the spectra, and a SUBCLASS field which displays values like ‘BROAD-

LINE’ or ‘STARFORMING’, but is often blank. For the ZWARNING field, I follow documented recommendations and accept only objects with ZWARNING of 0 (no warnings) or 16 (saturation) as well as 256 (poor astrometry for plughole) and some 128 (unplugged, but flag is documented to be wrong for about 200 objects which have strong signal). For the SUBCLASS field, I find from inspection of hundreds of spectra that the better quality spectra bear a populated SUBCLASS field, and the pipeline classifications and redshifts for those objects are of a good significance. In contrast, the spectra without a subclass are usually noisy and the pipeline information of a low significance—which undoubtedly explains the pipeline’s inability to discern a subclass. Accordingly, I take a populated SUBCLASS field to signal a high significance spectrum.

Thus, by use of the SUBCLASS and ZWARNING fields I am able to bulk-separate the pipeline-only quasars into high significance and low significance spectra, thus enabling inclusion of those high significance quasars into this catalogue. An additional benefit is that there is a high overlap of the SDSS3 data with the legacy SDSS data; thus all legacy pipeline-only quasars can be dropped unless qualifying by this SDSS3-based rule. However, pipeline-only quasars are also kept if confidently associated to radio/X-ray detections, even if the spectrum is of low significance. Also, pipeline-only redshifts above  $z = 4$  are excluded as per advice from Adam Myers; upon further inspection of high- $z$  pipeline-only spectra, I have lowered this cutoff to  $z = 3.65$ .

The total counts of SDSS-discovered type-1 objects included into HMQ are 369 249 manually checked quasars and 20 298 pipeline-only quasars. Also, 11 821 SDSS redshifts have been applied to quasars from earlier papers, the SDSS redshifts being favoured due to their precision and reliability. Specific breakdowns are available from the HMQ data in which each object is referenced with its discovery citation and redshift citation. Table 5 lists the discovery papers which contribute most quasars to the HMQ catalogue, in

**Table 5.** Top 25 discovery papers for the HMQ.

#	ID	# of type 1	# of redshifts	paper
1	SDSS DR12Q manual	154 958	298 959	Pâris et al. (2015)
2	SDSS DR9Q manual	62 478	218	Pâris et al. (2012)
3	SDSS DR10Q manual	58 006	808	Pâris et al. (2014)
4	SDSS DR3Q <sup>a</sup> manual	39 247	9	Schneider et al. (2005)
5	SDSS DR5Q manual	28 259	73	Schneider et al. (2007)
6	SDSS DR7Q manual	26 301	80 222	Schneider et al. (2010)
7	XDQSO candidates	23 135	0	Bovy et al. (2011)
8	2QZ/6QZ	23 036	19 692	Croom et al. (2004)
9	2SLAQ	7 722	6 556	Croom et al. (2009)
10	SDSS DR12 auto	4 261	5 781	Alam et al. (2015)
11	PGC <sup>b</sup>	4 254	5	Paturel et al. (2003)
12	SDSS DR8 auto	3 417	1 762	Aihara et al. (2011)
13	SDSS DR9 auto	2 952	2 770	Ahn et al. (2012)
14	SDSS DR3* auto	2 597	1 927	Abazajian et al. (2005)
15	SDSS DR10 auto	2 591	2 300	Ahn et al. (2014)
16	NBCKDE candidates	1 878	14 205	Richards et al. (2009)
17	SDSS DR7 auto	1 759	2 507	Abazajian et al. (2009)
18	DEEP2 Redshifts	1 437	1 400	Newman et al. (2013)
19		1 140	1 141	Iovino et al. (1996)
20	SDSS DR6 auto	1 043	1 487	Adelman-McCarthy et al. (2008)
21	SDSS DR4 auto	855	1 237	Adelman-McCarthy et al. (2006)
22	AGES survey	848	848	Kochanek et al. (2012)
23	SDSS DR5 auto	823	1 308	Adelman-McCarthy et al. (2007)
24	Magellanic Quasars	543	574	Kozłowski et al. (2013)
25	LAMOST Andromeda	519	455	Huo et al. (2013)

<sup>a</sup>DR3Q and DR3 here include the earlier DR1 and DR2 releases.

<sup>b</sup>The Principal Galaxy Catalogue (PGC) is not actually a discovery paper, but is used as a reference for names of AGN galaxies.

numerate order; there it is seen that the SDSS releases dominate the quasar portfolio today. A note on the Table 5 column ‘# of type 1’: this shows how many objects were originally presented by that paper, but SDSS astrometrically-based object names can change slightly between releases; the HMQ presents the current names of SDSS objects, so the discovery citation is that of the SDSS release which first presented the current name. My processing showed that DR12Q added 121 173 new type-1 quasars, so the 154 958 displayed in Table 5 includes 33 785 quasars with small name changes from earlier releases.

#### 4 NEW QUASARS

114 new quasars with spectral confirmation are presented in this catalogue. They are 92 quasars from Cyril Hazard’s work in the 1980s, 4 quasars from E. Margaret Burbidge (2003), and 18 quasars from Dan Weedman on a re-inspection of Weedman (1985). In detail:

1. 92 quasars from Cyril Hazard, the prominent early quasar researcher who identified many quasars from objective prism plates obtained with the UK Schmidt telescope in the 1980s Hazard (1980). Hazard’s *modus operandi* was to share his quasars out with other researchers rather than publish them himself. As a consequence, many remained unpublished. In June 2013, he

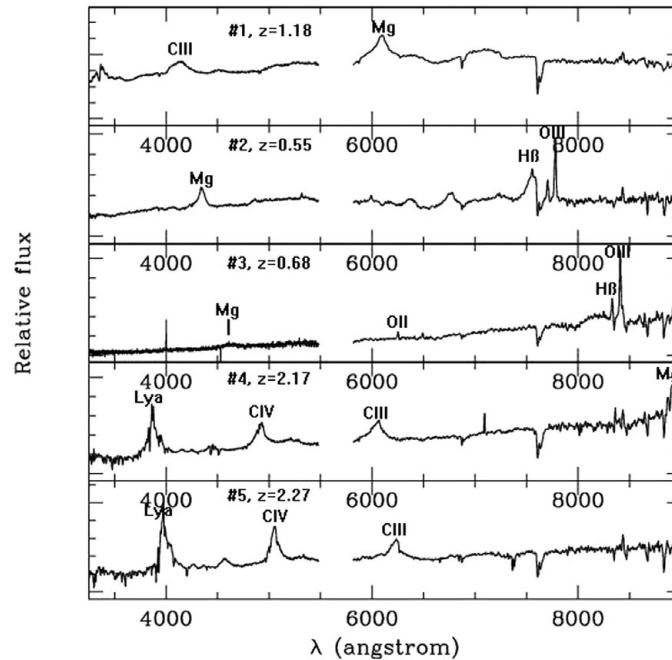
**Table 6.** Sample quasars from Cyril Hazard.

Name	J2000	Rmag	Bmag	z
HAZ 878	00 43 47.6 –26 54 16	18.5	18.7	1.290
HAZ R157	00 45 04.9 –21 53 01	18.2	18.0	2.766
HAZ 1113	00 46 35.3 –26 42 55	19.1	19.4	2.160
HAZ 0040+6	00 48 34.2 +07 53 44	18.6	18.9	2.800
HAZ R077	00 50 59.9 –24 11 38	18.2	18.7	2.958
HAZ 0120-3G	01 25 00.2 +04 01 48	18.6	19.6	2.100
HAZ 0128+01	01 31 18.9 +01 24 36	17.9	19.4	3.094
HAZ 62	04 49 03.2 –17 18 06	17.9	19.2	3.060
HAZ 12-5-43	12 09 35.2 +09 52 01	19.5	20.0	2.069
HAZ A136.1	14 58 45.2 +08 29 49	19.0	19.6	2.647

sent word that he is preparing a comprehensive presentation of his works, and we shared some data. These 92 new quasars were identified from that data, and Cyril graciously assented to their inclusion in this work. The quasar names are from his worksheets which I have prefaced with ‘HAZ’ to clarify their provenance; however, two objects had the same worksheet identifier of ‘122’, so I have renamed one as simply ‘HAZARD’. 24 of these objects have been covered by the subsequent SDSS DR12 release with all confirmed as quasars—these are readily identified in the catalogue by the redshift citation. A sample is shown in Table 6 and the

**Table 7.** Quasars from E. Margaret Burbidge (2003).

no.	Name	J2000	Rmag	Bmag	z	X-ray
1	CXO J02224+4221	02 22 24.4 +42 21 38	17.8	18.1	1.18	CXO J022224.4+422138
2	EMBUR 2	02 22 25.3 +42 24 50	20.3	21.0	0.55	CXO J022225.3+422450
3	EMBUR 3	02 22 32.6 +42 26 19	19.9	21.3	0.68	CXO J022232.6+422619
4	EMBUR 4	02 22 13.9 +42 25 16	19.5	20.3	2.17	3XMM J022213.9+422517
5	EMBUR 5	02 22 53.1 +42 13 06	19.5	19.6	2.27	3XMM J022253.1+421308

**Figure 2.** Spectra of the five Burbidge quasars, obtained with Keck-I LRIS using a 5600Å dichroic.

complete set can be extracted from the catalogue by selecting on names beginning with ‘HAZ’, or by the citation of Hazard (2013). Full information on these quasars and a larger set of work is in preparation by Cyril Hazard as of his last communication in September 2013.

- Four quasars from E. Margaret Burbidge, observed on the Keck-I LRIS on 2003 October 2. Six targets were selected via X-ray association in the vicinity of NGC 891, and five found to be quasars; the sixth (J022302.5+421731) was missed because the slit was mislaid onto two adjacent stars. Burbidge elected not to publish due to the sparse results, but released the material to associates, myself included. The five quasars are listed in Table 7 with X-ray associations. The spectra were reduced by C. Gutiérrez using IRAF<sup>7</sup> and are displayed in Figure 2 which I have annotated with line identifications. The first quasar has since

been re-surveyed by the Serendipitous Extragalactic X-ray Source Identification program (SEXSI: Eckart et al. 2006), so the remaining four are newly published here. I have named them as EMBUR 2 (etc.) after the discoverer, and their citation is Burbidge (2003).

- 18 quasars with probable redshifts from Dan Weedman. These were first presented in Weedman (1985) but without redshifts because each showed only a single emission line which could not be securely identified as Ly $\alpha$  or CIII, etc. Today we have SDSS-based photometric redshifts for these 18, primarily from Richards et al. (2009), which have enabled unambiguous identifications of each single emission line on the premise that the photometric redshift is near to the true redshift. These quasars have names of WEE 35, WEE 49, etc., from the original paper, and have a redshift citation of D. W. Weedman (2014, private communication) except for three re-surveyed by DR12 which confirm these as quasars.

<sup>7</sup>IRAF is the Image Reduction and Analysis Facility, <http://iraf.noao.edu>



**Table 8.** Counts of Radio/X-ray associations in the HMQ.

Object class	Total # objs	# X-ray	Core radio	Double lobes	Extra X-ray	Extra radio
QSOs	424 748	29 086	21 955	1 652	9 774	10 538
AGN	26 623	6 194	5 394	256	2 904	2 283
Photometric	25 015	16 954	8 336	438	4 281	4 285
BL Lac type	1 595	995	1 430	13	605	767
Type 2	32 783	2 419	4 697	271	860	1 822
ALL	510 764	55 648	41 812	2 630	18 424	19 695

## 5 CLASSIFICATION OF THE PRESENTED OBJECTS

There are five object classes reported in this catalogue which are shown with their counts in the first two columns of Table 8. Type 1 objects (class='Q' and 'A') are the main thrust of this catalogue and only high confidence objects with secure redshifts are included; where the discovery paper flags objects as questionable, those are dropped. SDSS quasars are included when presented by the manual surveys such as DR12Q, and also good confidence pipeline-only quasars are accepted as detailed in Section 3. However, the SDSS pipeline uses a 'BROADLINE' subclassifier for broadline emitters, so emitters not flagged as 'BROADLINE' are either narrow-line emitters or the spectrum was too low confidence to make a judgement. Therefore, to include pipeline-only quasars as type-1 objects, I require them to be either of good confidence with the 'BROADLINE' subclass, or of low confidence (i.e., blank subclass) with secure radio/X-ray association.

Type 2 objects (class='K') are included for user reference at  $\approx 90\%$  completeness from the literature, and are generally taken as narrow-line emitters although legacy usage varied. Also added are a selection of objects from the large SDSS releases which did not classify type 2 objects but included emitters not subclassed as 'BROADLINE', many of which will be type-2 objects. I used rules to include them as follows: firstly, 1 264 good confidence pipeline-only quasars not flagged as 'BROADLINE' were taken. Also, 1 089 manual quasars with those same attributes were taken, because the manual catalogues included but did not classify type-2 objects, see Pâris et al. (2012), introduction, last paragraph. Next, 16 842 SDSS galaxies subclassed as 'AGN' but not 'BROADLINE' were taken as narrow line Seyferts although some will be LINERS; similarly, 3 247 SDSS galaxies subclassed as 'AGN BROADLINE' were taken up as AGN (class='A'). These 20 089 galaxy sourced objects are flagged in the HMQ comment field with an 'a' to signal their provenance. In this way, the germane active objects from the SDSS releases have been included, although the HMQ class='K' consequently contains unquantified contamination from broadline quasars and LINERS.

BL Lac objects (class='B') have been quality checked and ones without radio/X-ray association which VCV an-

notated as 'BL?' have been dropped. Newly surveyed such objects are usually presented as 'candidates', so I have added those where confirmed by radio/X-ray association. There is an online compendium of blazars, the BZCAT Massaro et al. (2009) which has been used as a check and a reference, but not as a definitive guide.

The AGN (class='A') are in principle broadline Seyfert galaxies which are optically dominated by their disk, with QSOs (class='Q') being core-dominated objects with no disk seen. Of course the actual data shows intermediate objects throughout the full range, in line with the unified model. No attempt is made to subclass the AGN as S1.2, S1.5, etc. VCV used a cosmology-based luminosity threshold to separate the AGN and QSOs, and re-released their final edition with a changed cosmology. By contrast, the approach here is simply a practical one to separate the visually extended AGN from the unresolved QSOs, analyse those groups to get a luminosity based divider, and extend that divider into the set of fainter unresolved objects. If done correctly, the separator should trace a path from the bright QSO-AGN divider to some natural break in the bulk fainter data profile as is seen in Figure 3. With some testing I have identified a simple luminosity equation

$$magnitude = 22 + 5 \times \log_{10}(z \times (1 + z)),$$

which traces the required path. However, type 1 objects of  $z < 0.1$  (as a rough cut) are all taken as AGN Seyferts, consistent with the absence of nearby quasars. Thus, I need to adjust the separator to terminate at  $z = 0.1$ . Doing so gives the following:

$$magnitude = 22 + 5 \times \log_{10}(z \times (0.8 + z) - 0.09),$$

as the separator which is bounded by  $V_{mag} = 17.0$  at  $z = 0.1$ . However, such bright objects can be classified by their psf. The separator is needed for the set of objects which are psf-unresolved just because they are so faint; these are SDSS objects with  $g \geq 22.0$  ('survey-quality threshold', Pâris et al. 2014, Section 2.3) and  $V_{mag} \geq 21.0$  for other objects. The separator is also needed for brighter objects which have no psf class, e.g., USNO-B photometry. This luminosity-based separator equation is that of a static Euclidean manifold with time dilation, so is non-physical in a scale-invariant universe, but fits the data well. Figure 3 shows the separator at  $x=0$  as a local minimum in the data profile of the faint objects. The

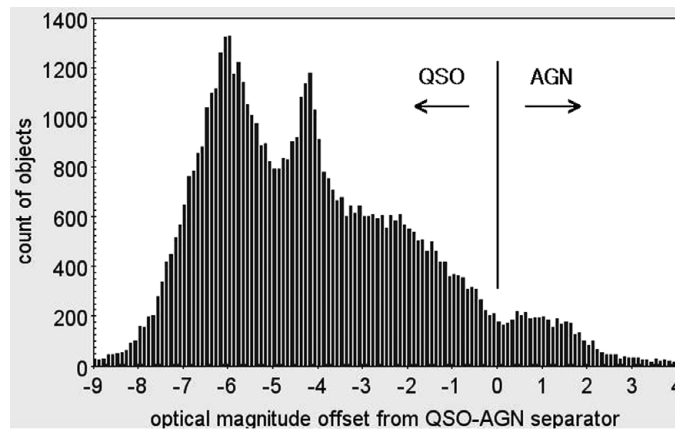


**Figure 3.** Vmag offsets from luminosity separator for faint (see text) or no-psf type-1 objects, binned by 0.1 mag. Chart produced with TOPCAT (Taylor 2005).

QSOs to the left (brighter) of the separator comprise the bulk of the objects; the twin peaks are an artefact of SDSS BOSS<sup>8</sup> selection. The AGN to the right (fainter) of the separator have a Gaussian-looking profile which, if real, implies some underlying physical distinction between the QSOs and AGN.

In summary of type 1 objects, extended psf morphology signals an AGN, with SDSS morphology used for SDSS photometry. Galaxies from the Principal Galaxy Catalogue Paturel et al. (2003) are taken as extended, as well as any type-1 of  $z < 0.1$ . Brighter unresolved objects (as defined above) are classified as QSO, and fainter unresolved objects, and those without psf class, are classified as QSO or AGN using the above separator equation; the overall outcome is  $\approx 94\%$  QSOs.

## 6 OPTICAL PHOTOMETRY

The HMQ sources optical photometry from a background data pool as is documented in Flesch & Hardcastle (2004), but some points are worth highlighting. The optical data is presented as red and blue psf and magnitudes, and are preferentially sourced from Cambridge Automatic Plate Measuring machine (APM) McMahon & Irwin (1992) and United States Naval Observatory Monet et al. (2003) USNO-B data. In particular, their data from the first-epoch National Geographic-Palomar Observatory Sky Survey (POSS-I) are preferred because POSS-I *O* is violet 4 100Å and so well-offset from POSS-I *E* 6 500Å and both plates were always taken on the same night, thus the red–blue colour is correct even for variable objects. Other surveys’ photometry are used where POSS-I data is incomplete, and SDSS photometry is used where both red and blue magnitudes are not already available from the APM or USNO-B. The HMQ ReadMe has additional information about the photometry and how it is flagged in the data.

<sup>8</sup>Baryon Oscillation Spectroscopic Survey, <http://www.sdss3.org/surveys/boss.php>

## 7 RADIO AND X-RAY ASSOCIATIONS

HMQ displays radio/X-ray associations just by giving the radio/X-ray identifier(s) without elaboration. Beneath this simple presentation are the calculations detailed in Flesch & Hardcastle (2004) which quantify causality, i.e., the confidence that the association is true. In brief, the method is that areal densities of optical profiles around radio/X-ray detections are compared to background averages to obtain the causality percentage. These calculations are done against anonymous optical data, and catalogues like the Atlas of Radio/X-ray Associations Flesch (2010) which report associations to anonymous optical objects do need to display those calculated probabilities. But when that anonymous object turns out to be a quasar, which are commonly radio/X-ray emitters, then that is a strong confirmation that the association is correct. Thus, since HMQ has quasars only, this very simple presentation style can be used.

The radio/X-ray associations were useful in making many identifications, e.g., the quasar ‘Q 1224-116’ is identified as the  $r = 18.3$   $b = 18.6$  object at 12 27 25.0-11 33 39 (J2000) because of the X-ray association 3XMM J122725.1-113340, whereas previously it was identified to the nearby galaxy 2MASSi J1227247-113334; the original author did not distinguish between them. This theme was encountered in many places.

The ReadMe itemises the radio/X-ray surveys used, but of course they are all the largest ones like the NRAO VLA Sky Survey catalog (NVSS: Condon et al. 1998), the Faint Images of the Radio Sky at Twenty-cm survey catalog (FIRST: White et al. 1997), and the Sydney University Molonglo Sky Survey Murphy et al. (2007) for the radio data, and *Chandra*, *XMM-Newton*, *Swift*, and *ROSAT* catalogues for the X-ray data. Optical field solutions are calculated from the raw source positions of all these catalogues as described in Flesch (2010). Radio and X-ray associations are calculated independently of each other.

The radio/X-ray identifiers are displayed in four columns which are one for X-ray, one for core radio, and two for

double radio lobes. Some association identifications are seen in the sample data of [Table 1](#) and [Table 8](#) shows the total HMQ count of association types by object class. However, radio lobes are uncommon (<1%), so when there are no lobes those two columns are instead used to display additional radio/X-ray identifiers from other surveys; this conveys a fuller sense of the data available. The README gives the rules used. The four columns are usually enough to display all available associations, but any overflow is not shown; this happens for 2 891 objects with a total of 4 241 X-ray associations dropped, representing 5.7% of all X-ray associations. An example is the blazar ‘ON 231’, seen in [Table 1](#) with 4 associations but has additional X-ray associations 2RXP J122132.0+281403, 1WGA J1221.5+2813 and 1RXS J122131.1+281402. Such extra identifiers would be nice to show but it is not essential because they all refer to the same physical X-ray source seen on the sky, so are duplicates in that sense.

## 8 INCLUSION OF PHOTOMETRIC QUASARS

This catalogue includes 25 015 high-confidence (99%) SDSS photometric quasar candidates which also show radio and/or X-ray associations. These objects are well assured of being true quasars because two independent procedures, the photometry calculations and the radio/X-ray association calculations, separately identify the same objects as likely quasars, and the calibrated joint calculation given below quantifies that to the 99% likelihood required.

These objects are within the scope of this catalogue because the confidence in the spectroscopically confirmed quasars, i.e., that they are true quasars, are also rated at about 99%. This assessment is based on historical performance, and three examples convey the point. First, the VCV quasar catalogue, heretofore the authoritative standard, was found above to have  $\approx 5$  000 galaxies or stars amongst its 168 941 nominal active objects for an error rate of 3% and thus performance of 97%. Those have been removed but an unquantified residue remains from legacy surveys. The second example is that of the 20 298 SDSS pipeline-only quasars, documented above, which are included because the preponderance of them are true quasars, but some noisy spectra are present which conceal an error rate which I can estimate only informally at about 5%. Thirdly, even the high-quality SDSS manual surveys have a typical drop rate of 0.15% per each new edition (Schneider et al. 2010, Section 6), and in the case of DR10Q which presented 169 459 QSOs, the subsequent DR12Q release reclassified 1 655 of those into galaxies and dropped 25 entirely, for a total 0.99% drop rate. So, false positives slip through even under state-of-the-art conditions. Thus, over the set of all classified quasars in the literature, my assessment of an overall 1% error rate is a fair call.

Accordingly, the confirmed objects can be supplemented with photometric candidates which as a group also have 99% confidence of being true quasars. These photometric quasars are from the SDSS-based NBCKDE (i.e., Nonparametric

Bayes classifier – kernel density estimate) Richards et al. (2009) and XDQSO (i.e., Extreme-deconvolution QSO targets) Bovy et al. (2011) photometric quasar candidate catalogues. These catalogues give nominal estimates of pQSO (probability of being a true QSO) for each object which however are not calibrated against confirmed classified objects. I have performed that calibration against DR12Q classifications, and the details of that calibration and discussions of the NBCKDE and XDQSO attributes are in [Appendix A](#). This yields a calibrated photometrically-based QSO likelihood for each candidate.

Next, QSO likelihoods are needed for the radio/X-ray associations. The calculations described in [Section 7](#) obtain the confidence of association percentage, i.e., causality, and the classified objects used in that analysis include a percentage of QSOs; thus, causality  $\times$  QSO% = QSO likelihood. This likelihood is already calibrated against confirmed objects as part of the calculation. Double radio lobes are included via a heuristic algorithm, also calibrated.

Now the calibrated photometric based QSO likelihood  $P_1$  and the radio/X-ray association based QSO likelihood  $P_2$  are combined as (expressing the likelihoods as fractions)

$$P_{\text{tot}} = 1/(1 + ((1 - P_1)(1 - P_2)/P_1P_2)),$$

This equation requires a component to be above 50% for it to make a positive contribution to the outcome; therefore we consider only objects with both  $P_1 > 50\%$  and  $P_2 > 50\%$ . The goal is to identify the set of candidates with  $P_{\text{tot}} \geq 99\%$ . [Table 9](#) shows the result, binned by rounded  $P_{\text{tot}}$ , and the three right-hand columns show the results for fellow candidates which have since been classified by SDSS-DR12Q (with ZWARNING=0 for best precision). Column 6 gives the actual QSO percentage of classified objects, and shows a performance break between the rows binned at 96% and 97%, so I provisionally accept the bins of 97% to 100% (i.e., the bottom 4 rows) as equivalent actual performers, and sum them at bottom. For that total set, the column 3 calculated likelihood is 98.977% which is acceptably close to the 99% criterion, and the column 6 actual QSO percentage of 99.175% meets the criterion. In this way, the 25 015 are selected.

These 25 015 photometric objects are given class=‘q’ in this catalogue to identify them as objects without full spectra, but photometric redshifts are displayed. These are sourced as available from NBCKDE which provides redshifts for 14 202 NBCKDE-only and shared objects. The remaining 10 813 objects are XDQSO-only, but XDQSO has not published photometric redshifts. These I have calculated via a clustering method akin to rainfall analysis which is described in [Appendix B](#). Note that photometric redshift calculations sometimes fail to achieve a result, for example when two contending redshift values are adjudged equally likely. This was the case for an additional 627 otherwise-qualifying candidates, representing a failure rate of 2.4%, which were accordingly excluded from the HMQ because redshifts are required. All photometric redshifts are rounded to 0.1  $z$  in

**Table 9.** QSO likelihoods for the SDSS candidates, with confirmed percentages.

$P_{\text{tot}}$ bin	Candidate # objects	$P_{\text{tot}}$ avg pct	DR12Q # objjs	DR12Q # QSOs	DR12Q QSOpct
90%	403	90.024	63	62	98.413
91%	492	91.018	85	82	96.471
92%	580	92.038	102	99	97.059
93%	703	93.041	159	155	97.484
94%	873	94.031	162	160	98.765
95%	1 164	95.035	225	217	96.444
96%	1 575	96.030	334	326	97.605
97%	2 464	97.044	475	471	99.158
98%	4 267	98.055	840	828	98.571
99%	8 286	99.065	2 069	2 059	99.517
100%	9 998	99.774	3 041	3 014	99.112
97–100	25 015	98.977	6 425	6 372	99.175

the catalogue to help convey that they are estimates. Sample objects are seen at top and bottom rows of [Table 1](#).

## 9 MISCELLANEOUS NOTES

The HMQ includes 6 770 new spectroscopically confirmed QSOs (and 4 560 type-2) from 101 papers published since the VCV 13th edition, apart from the SDSS surveys. My thanks to those authors who sent me lists of their objects. Also, 180 QSOs from 67 early papers overlooked by VCV have also been added.

The biggest ongoing task throughout this project was de-duplication of objects across papers and surveys, while preserving true doublets. These are all resolved except maybe for two BL Lac objects (or is it one) which are SHBL J23435+3440 at J234333.8+344005 and BZBJ2343+3439 at J234333.5+343948. These objects are 14 arcsec apart, and both have  $z=0.336$ . The SHBL object has radio NVSS J234333.7+344000 and the BZB object has X-ray 1SXPS J234333.4+343949. The BZB object has white BL Lac colours while the SHBL object is quite red, but its discovery paper was clear on the identification. I suspect the SHBL object is the true one and the BZB object a duplicate, but possibly both are valid so both are in this catalogue.

The HMQ is a catalogue of quasars and not of gravitational lens images, so I have de-duplicated multiple lensed signatures into single identifications where I was aware of them; the optically brightest signature is the one retained.

I write NVSS radio detections in the form *NVSS Jhh-mmss.s+ddmmss* which is the standard form used by radio/X-ray surveys, although the recommended NVSS naming convention is *NVSS Jhhmmss+ddmmss*. I prefer the standard form because when both FIRST and NVSS report the same signature, their astrometry agrees well, often to the arcsecond, so the standard form displays useful astrometric information. The recommended NVSS name can be recovered by simply removing the time decimal.

PASA, 32, e010 (2015)  
doi:[10.1017/pasa.2015.10](https://doi.org/10.1017/pasa.2015.10)

## 10 CONCLUSION

The HMQ catalogue is presented as a comprehensive edition, complete to 2015 January 25, which displays 451 371 type 1 QSOs and AGN, 25 015 high-confidence photometric quasars, 1 595 BL Lac objects, and 32 783 type 2 objects. Astrometry is arcsecond accurate for most objects, out to 2 arcsec precision for some legacy objects. X-ray and radio associations for these quasars are presented as applicable, including double radio lobes. Issues of identification and classification have been resolved to where the full quasar portfolio can be easily integrated into large databases.

## ACKNOWLEDGEMENTS

Thanks to NASA HEASARC for putting an early version of this catalogue online which motivated me to clean up all the issues with it, although I had no idea that it would take me five years to do so. Thanks to Dave Monet for generously providing USNO-B optical data. Thanks to Steve Willner for finding papers which I could not. Emanuele Farina for keeping me on my toes with some early duplicates, and to Isabelle Pâris for helpful discussions. Thanks to the sci.astro.research newsgroup, astutely moderated by Martin Hardcastle, which gave me a platform to hammer out issues and get valuable feedback. This work was not funded.

## REFERENCES

- Abazajian, K. N., et al. 2005, AJ, 129, 1755, SDSS DR3  
 Abazajian, K. N., et al. 2009, ApJS, 182, 543, SDSS DR7  
 Adelman-McCarthy, J. K., et al. 2006, ApJS, 162, 38, SDSS DR4  
 Adelman-McCarthy, J. K., et al. 2007, ApJS, 172, 634, SDSS DR5  
 Adelman-McCarthy, J. K., et al. 2008, ApJS, 175, 297, SDSS DR6  
 Ahn, C. P., et al. 2012, ApJS, 203, 21, SDSS DR9  
 Ahn, C. P., et al. 2014, ApJS, 211, 17, SDSS DR10  
 Aihara, H., et al. 2011, ApJS, 193, 29, SDSS DR8  
 Alam, S., et al. 2015, arXiv 1501.00 963, SDSS DR12  
 Barcons, X., et al. 2007, A&A, 476, 1191, XMSS  
 Bovy, J., et al. 2011, ApJ, 729, 141, SDSS-XDQSO  
 Burbidge, E. M. 2003, unpublished, October 2003 Keck-I LRIS  
 Colless, M., et al. 2001, MNRAS, 328, 1039, 2dF-GRS

- Condon, J. J., Cotton, W. D., Greisen, E. W., Yin, Q. F., Perley, R. A., Taylor, G. B., & Broderick, J. J. 1998, *AJ*, 115, 1693
- Croom, S. M., Smith, R. J., Boyle, B. J., Shanks, T., Miller, L., Outram, P. J., & Loaring, N. S. 2004, *MNRAS*, 349, 1397, 2QZ/6QZ
- Croom, S. M., et al. 2009, *MNRAS*, 392, 19, 2SLAQ
- Cupani, G., Cristiani, S., D'Odorico, V., Milvang-Jensen, B., & Krogager, J.-K. 2011, *A&A*, 529, 99
- Eckart, M. E., Stern, D., Helfand, D. J., Harrison, F. A., Mao, P. H., & Yost, S. A. 2006, *ApJS*, 165, 19
- Edwards, G., Beauchemin, M., & Borra, E. F. 1988, *PASP*, 100, 266
- Flesch, E. 2010, *PASA*, 27, 283, ARXA
- Flesch, E. 2013, *PASA*, 30, 4
- Flesch, E., & Hardcastle, M. J. 2004, *A&A*, 427, 387, Quasars.Org catalogue (QORG)
- Gaston, B. 1983a, Ph.D thesis (University Park, PA: Pennsylvania State University)
- Gaston, B. 1983b, *ApJ*, 272, 411
- Ge, J.-Q., Hu, C., Wang, J.-M., Bai, J.-M., & Zhang, S. 2012, *ApJS*, 201, 31, Double-Peaked NELGs
- Hazard, C. 1980, In: Variability in Stars and Galaxies. Proc. 5th European Regional Meeting in Astronomy (Liege: Institut d'Astrophysique), GL.2.1
- Hazard, C. 2013, in preparation
- Huo, Z.-Y., et al. 2013, *AJ*, 145, 159, LAMOST Andromeda pilot
- Iovino, A., Clowes, R., & Shaver, P. 1996, *A&AS*, 119, 265
- Kleinman, S. J., et al. 2013, *ApJS*, 204, 5, SDSS DR7 WDs
- Kochanek, C. S., et al. 2012, *ApJ*, 200, 8, AGES survey
- Kozłowski, S., et al. 2013, *ApJ*, 775, 92, Magellanic Quasars
- La Franca, F., Lissandrini, C., Cristiani, S., Miller, L., Hawkins, M. R. S., & McGillivray, H. T. 1999, *A&AS*, 140, 351
- Massaro, E., Giommi, P., Leto, C., Marchegiani, P., Maselli, A., Perri, M., Piranomonte, S., & Scavi, S. 2009, *A&A*, 495, 691, BZCAT v4.1.1 (2012), <http://www.asdc.asi.it/bzcat>
- Mauch, T., & Sadler, E. M. 2007, *MNRAS*, 375, 931
- McMahon, R. G., & Irwin, M. J. 1992, in Digitised Optical Sky Surveys, ed. H. T. MacGillivray & E. B. Thomson (Dordrecht: Kluwer), 417 (APM)
- Monet, D. G., et al. 2003, *AJ*, 125, 984 (USNO-B)
- Murphy, T., Mauch, T., Green, A., Hunstead, R. W., Piestrzynska, B., Kels, A. P., & Sztajer, P. 2007, *MNRAS*, 382, 382
- Newman, J. A., et al. 2013, *ApJS*, 208, 5, DEEP2 Redshifts
- Pâris, I., et al. 2012, *A&A*, 548, 66, SDSS DR9 Quasar
- Pâris, I., et al. 2014, *A&A*, 563, 54, SDSS DR10 Quasar
- Pâris, I., et al. 2015, in preparation, SDSS DR12 Quasar
- Paturel, G., Petit, C., Prugniel, Ph., Theureau, G., Rousseau, J., Brouty, M., Dubois, P., & Cambrésy, L. 2003, *A&A*, 412, 45, Principal Galaxy Catalogue
- Richards, G. T., et al. 2009, *ApJS*, 180, 67, NBCKDE
- Sandage, A., & Bedke, J. 1994, *The Carnegie Atlas of Galaxies*, Vol. 1, No. 638 (Washington, DC: Carnegie Institution)
- Schneider, D. P., Schmidt, M., & Gunn, J. E. 1994, *AJ*, 107, 1245
- Schneider, D. P., Schmidt, M., & Gunn, J. E. 1999, *AJ*, 117, 40
- Schneider, D. P., et al. 2005, *AJ*, 130, 367, SDSS DR3 Quasar
- Schneider, D. P., et al. 2007, *AJ*, 134, 102, SDSS DR5 Quasar
- Schneider, D. P., et al. 2010, *AJ*, 139, 2360, SDSS DR7 Quasar
- Taylor, M. B. 2005, *ASPC*, 347, 29, TOPCAT software
- Véron-Cetty, M.-P., & Véron, P. 2010, *A&A*, 518A, 10
- Weedman, D. W. 1985, *ApJS*, 57, 523
- White, R. L., Becker, R. H., Helfand, D. J., & Gregg, M. D. 1997, *ApJ*, 475, 479

*PASA*, 32, e010 (2015)  
doi:10.1017/pasa.2015.10

## APPENDICES

### A PHOTOMETRIC LIKELIHOOD CALIBRATION

The HMQ includes 25 015 photometric quasars from the SDSS-based XDQSO Bovy et al. (2011) and NBCKDE Richards et al. (2009) photometric quasar candidate catalogues. These are a small fraction of the total objects from these catalogues. XDQSO data consists of 160M objects in 39Gb of files, most of which are stars, and provides a nominal pQSO (percentage chance of being a QSO) which their paper cautions is just a comparative figure and not a genuine QSO likelihood (see esp. their Figure 14). The primary purpose of XDQSO was to select targets for the SDSS BOSS campaign, and those are flagged with good = 0 (which means good). Those not so flagged could still have a high pQSO but would have deficiencies such as being optically too faint, etc. 3 010 139 XDQSO candidates have pQSO > 0.5 of which 1 792 678 were BOSS targets and 1 217 461 were non-BOSS. NBCKDE's final release was as a file of 1 015 082 'most robust' candidates, with the pQSO presented as comparative QSO and star density logarithms; 992 700 of these have pQSO > 0.5.

To get best use of the pQSOs, it is desirable to calibrate them such that they represent the true odds of the candidate being a QSO (the 'QSO<sub>pct</sub>'). The subsequent SDSS BOSS releases DR9-DR12 were of course largely onto targets selected by XDQSO and NBCKDE, so a large pool of spectroscopically classified objects are available to reconcile to; the SDSS-DR12Q Pâris et al. (2015) superset has 531 648 manually classified quasars, stars, and galaxies, of which 331 188 were XDQSO BOSS targets, 170 145 were NBCKDE candidates, and 7 289 were XDQSO non-BOSS objects. However, there is extensive overlap between XDQSO and NBCKDE, and in the calibration exercise it is desirable to separate them lest objects be double-counted which would denormalise the calibration. Germane to this is that the NBCKDE footprint (DR6 based) is completely within the XDQSO footprint (DR8 based), so removal of the shared objects will still allow NBCKDE to be treated as an internally consistent dataset. Therefore, the 331 188 XDQSO BOSS targets are processed as the first priority, while just 24 127 NBCKDE candidates not matching to BOSS remain as the second group to be processed. However, the performance of the complete NBCKDE data is interesting in its own right, and will be analysed below also.

Of the 7 289 non-BOSS XDQSO objects classified by DR12Q, 4 169 are shared with NBCKDE but are left to be processed with the NBCKDE group. This is because the vast majority of non-BOSS objects are optically very faint or have photometry issues, and the subset classified by DR12Q were picked from the more eligible members, thus not very representative of the whole group. Exclusion of the NBCKDE-shared objects lowers the QSO percentage of the remaining 3 120 non-BOSS candidates more to what is expected for the group as a whole. Thus the 3 120 non-BOSS XDQSO objects which are not shared with NBCKDE are the final group to be processed.

The calibration procedure is presented as two tables, and each table presents figures for four groups of candidates, being (1) XDQSO BOSS, (2) NBCKDE full set, (3) NBCKDE-only candidates (not shared with BOSS), and (4) XDQSO non-BOSS candidates which are not shared with NBCKDE. Table A1 shows the performance of the nominal pQSOs for each group when compared to the DR12Q-revealed classifications. The pQSOs are binned by 5% in the range 60% to 85% (with the displayed figure being the midpoint of the

**Table A1.** Before Calibration: XDQSO/NBCKDE pQSOs compared to DR12Q superset QSO pcts.

pQSO bin	XDQSO BOSS targets				NBCKDE full data				NBCKDE-only data <sup>a</sup>				XDQSO non-BOSS <sup>b</sup>			
	DR12Q #objs	DR12Q #QSOs	DR12Q QSO pct	calib bin	DR12Q #objs	DR12Q #QSOs	DR12Q QSO pct	calib bin	DR12Q #objs	DR12Q #QSOs	DR12Q QSO pct	calib bin	DR12Q #objs	DR12Q #QSOs	DR12Q QSO pct	calib bin
60	16 063	7963	49.6	46	1227	848	69.1	48	423	215	50.8	24	233	145	62.2	60
65	16 571	8813	53.2	51	4164	2264	54.4	53	1849	707	38.2	29	204	126	61.8	62.5
70	17 223	9793	56.9	56	6190	3612	58.4	58	2353	932	39.6	34	206	142	68.9	65
75	18 405	11202	60.9	61	7358	4647	63.2	63	2213	860	38.9	39	185	130	70.3	67.5
80	20 251	13176	65.1	66	10 423	7054	67.7	68	2589	1139	44.0	44	216	154	71.3	70
85	22 903	16171	70.6	71	13 157	9426	71.6	73	2359	1091	46.2	49	193	145	75.1	72.5
88	5147	3771	73.3	74	3119	2341	75.1	76	479	255	53.2	52	48	37	77.1	74
89	5500	4116	74.8	75	3501	2644	75.5	77	518	238	45.9	53	44	37	84.1	74.5
90	5780	4394	76.0	76	3924	3090	78.7	78	502	267	53.2	54	36	25	69.4	75
91	6082	4791	78.8	78	4446	3532	79.4	80	464	263	56.7	55	39	31	79.5	75.5
92	6628	5235	79.0	80	5108	4150	81.2	82	516	285	55.2	56	31	22	71.0	76
93	7355	6005	81.6	82	6606	5520	83.6	84	603	356	59.0	61	46	38	82.6	76.5
94	8145	6804	83.5	84	9334	7983	85.5	86	732	463	63.3	66	45	35	77.8	77
95	9303	7959	85.6	86	13 782	12258	88.9	88	832	605	72.7	71	44	31	70.5	77.5
96	11 022	9714	88.1	88	16 565	15084	91.1	90	983	774	78.7	76	62	46	74.2	78
97	13 424	12085	90.0	90.5	16 749	15477	92.4	92	1100	923	83.9	81	49	37	75.5	78.5
98	17 977	16742	93.1	93	17 426	16251	93.3	94	1536	1337	87.0	86	92	70	76.1	79
99	29 662	28319	95.5	95.5	15 323	14628	95.5	96	1767	1624	91.9	91	119	96	80.7	79.5
100(hw)	38 961	37452	96.1	97.4	9056	8741	96.5	97.5	1141	1058	92.7	94.8	197	101	51.3	79.9
ALL	331 188	238 470	72.0		170 145	141 240	83.0		24 127	13959	57.9		3120	2009	64.4	

<sup>a</sup>data not shared with XDQSO BOSS<sup>b</sup>data not shared with NBCKDE

bin), then binned by 1% in the range 88% to 100%; this highlights the high percentage bins which have the most numbers and the best performance.

For each group, the ‘DR12Q QSO<sub>pct</sub>’ column is the calibrator; we want a mapping which will convert the pQSO (i.e., the nominal QSO expectancy) to that QSO<sub>pct</sub> (i.e., the calibrated actual performance), but it needs to be a simple mapping to smooth the outcome. I have used these simple mappings to achieve the calibration

1. XDQSO BOSS targets:
  - for  $pQSO \leq 90$ :  $QSO_{pct} = pQSO - 14$
  - for  $90 < pQSO \leq 96$ :  $QSO_{pct} = 2 \times pQSO - 104$
  - for  $pQSO > 96$ :  $QSO_{pct} = 2.5 \times pQSO - 152$
2. NBCKDE full data:
  - for  $pQSO \leq 90$ :  $QSO_{pct} = pQSO - 12$
  - for  $pQSO > 90$ :  $QSO_{pct} = 2 \times pQSO - 102$
3. NBCKDE-only data:
  - for  $pQSO \leq 92$ :  $QSO_{pct} = pQSO - 36$
  - for  $pQSO > 92$ :  $QSO_{pct} = 5 \times pQSO - 404$
4. XDQSO non-BOSS data:
  - $QSO_{pct} = 30 + pQSO/2$

These mappings converts the pQSO bin to the calibrated QSO<sub>pct</sub> value displayed in the column ‘calib bin’. Table A2 shows this same data when binned by these calibrated QSO<sub>pct</sub>s, so we can better inspect the outcome. The smoothed QSO<sub>pct</sub> bin at left should ideally match the ‘DR12Q QSO<sub>pct</sub>’ column value in each of the four groups of candidates; in practice, the XDQSO BOSS and full NBCKDE data are well-fit, the NBCKDE-only data is adequately fit, and the XDQSO non-BOSS data is only marginally fit but the numbers are small. These tables do not show the low-pQSO bins where the numbers are small and the calibrations are ill-fitting and not useful, but those poorly performing objects are not of interest to this exercise. The calibration shows the effect of removing the XDQSO-shared objects from the NBCKDE data: the NBCKDE-only pQSOs are about 15% less well performed than the full NBCKDE pQSOs, showing that the shared objects were the best targets. For the full catalogues, the NBCKDE and XDQSO BOSS pQSOs have similar performance, NBCKDE being very slightly the better performed.

The full listing of 358 435 SDSS-DR12Q superset classified objects and the XDQSO and NBCKDE pQSOs for them is available for inspection<sup>9</sup>. Thus in this way, the XDQSO and NBCKDE pQSOs are calibrated into true QSO<sub>pct</sub>s, thus enabling the calculations of Section 8 which yield the additional 25 015 objects for the HMQ catalogue.

## B PHOTOMETRIC REDSHIFTS MADE EASY

Statistical tasks can be made easy if a large training set is available and the data is well defined. So, it was for me when I first calculated photometric redshifts for the XDQSO BOSS candidates, because the SDSS-DR9 provided 199 751 quasar redshifts as a training set. I have now recalculated these using 386 303 quasar redshifts from the DR12Q manual catalogue, which of course yields little change since the DR9 training set was already very large.

SDSS photometry is of five bands known as *ugriz* with mid-points at approx 3 600Å, 4 800Å, 6 200Å, 7 600Å, and 9 000Å,

respectively. These magnitudes provide four colours: *ug* ( $=u-g$ ), *gr*, *ri*, and *iz*. My procedure is to class each candidate by those colours (rounded to 0.1 mag), and the training set provides spectroscopic redshifts for all classified quasars having those same colours. So for a candidate having colours  $\{ug = 0.2 \text{ } gr = 0.2 \text{ } ri = -0.1 \text{ } iz = 0.4\}$ , the profile of spectroscopically confirmed redshifts is shown in Figure B1.

The colour-fitting training set objects are supplemented by near-colour fits (e.g., perturbing each colour in turn by 0.1 mag) which are weighted much less, so that candidates with unusual colour profiles will still have an adequate pool of training set objects. The task now is to reduce this redshift profile into a single photometric redshift value—basically, the redshift value with the greatest expectancy of success which we arbitrarily define as being within 0.5 *z* of the true spectroscopic redshift; however, closer precision is always a goal. The method is to cluster the redshift bins, identify the largest cluster, and select the redshift from that cluster.

NBCKDE Richards et al. (2009) used a kernel density estimate to cluster their training set data, and selected the ‘most likely’ photometric redshift as the weighted average of the bounded maximal cluster for each candidate. In this work, for simplicity, I use a variant of the ‘rainflow’ method which is used in engineering to cluster a continuous record (usually of amplitudes  $\times$  time) into a series of discrete events. Rainflow analysis requires both a peak maximum and peak minimum to define an event; it is a form of profile reduction. I apply such an algorithm to the redshift profile of Figure B1; the result is seen on Figure B2 upper left, where the 4 vertical dividers delineate the 5 clusters identified by the rainflow algorithm. The clusters are summated and the 2nd cluster centred on  $z = 0.9$  is identified as the largest, and its largest single bin (of width 0.1 *z*) is selected as the photometric redshift; thus the rainflow value is  $z = 0.9$ . The NBCKDE photometric redshift for this object is 0.845, the difference being from different cluster boundaries and that NBCKDE used the weighted average of the cluster; I prefer to use the maximum bin value in view of that cluster boundaries are not always clear. This object is identified in Figure B2 as SDSS J000922.96+155201.8 and it is a DR12Q object (as all of these are) with a spectral redshift of 1.012.

Figure B2 shows a brief sample of redshift profiles encountered in this task. The upper-right profile is for objects of colours  $ug = 0.4 \text{ } gr = 0.0 \text{ } ri = 0.3 \text{ } iz = 0.1$  and shows three clusters;  $z = 0.6$  is selected as the photometric redshift. NBCKDE selected  $z = 1.625$ , evidently because they treated the grouping on the right as a single cluster, whereas the rainflow algorithm divided it. That the spectral redshift is 0.601 is of no moment; quasars of the same colours with spectral redshift of 1.6 or 1.7 are trivially found.

Figure B2 middle-left has colours  $ug = 1.8 \text{ } gr = 0.2 \text{ } ri = 0.1 \text{ } iz = 0.0$  and is obviously a high-redshift object where the Lyman break enters the optical domain and dims the *u* magnitude. No clustering to be done, so my photometric redshift is 3.1, NBCKDE has 3.045, spectral is 3.348.

Figure B2 middle-right has colours  $ug = 0.4 \text{ } gr = 0.2 \text{ } ri = 0.2 \text{ } iz = 0.0$  and shows two obvious clusters. My photometric redshift is 1.5, NBCKDE has 1.465, spectral is 1.480.

Figure B2 lower left has colours  $ug = -0.1 \text{ } gr = -0.2 \text{ } ri = 0.3 \text{ } iz = 0.1$  and shows five clusters of which the one on the right is obviously the ‘winner’. My photometric redshift is 1.8, NBCKDE has 2.025, spectral is 1.898. The low counts (vertical axis) show that this colour profile is unusual, and the fractional counts show that the training set was supplemented by perturbed values having small weights.

<sup>9</sup>at <http://quasars.org/photometric-DR12Q.txt> (25Mb file)

**Table A2.** After Calibration: XDQSO/NBCKDE QSOpts compared to DR12Q superset QSOpts.

QSOpt bin	XDQSO BOSS targets			NBCKDE full data			NBCKDE-only data <sup>a</sup>			XDQSO non-BOSS <sup>b</sup>		
	DR12Q #objs	DR12Q #QSOs	DR12Q QSOpt	DR12Q #objs	DR12Q #QSOs	DR12Q QSOpt	DR12Q #objs	DR12Q #QSOs	DR12Q QSOpt	DR12Q #objs	DR12Q #QSOs	DR12Q QSOpt
60	18 303	10945	59.8	6586	3977	60.4	590	345	58.5	441	275	62.4
65	19 632	12615	64.3	8362	5472	65.4	716	440	61.5	414	287	69.3
70	22 268	15482	69.5	11 406	7850	68.8	820	599	73.0	398	280	70.4
75	22 843	17007	74.5	14 994	11061	73.8	976	770	78.9	405	315	77.8
80	16 698	13333	79.8	12 333	9848	79.9	1079	892	82.7	537	362	67.4
85	21 859	18489	84.6	20 720	17617	85.0	1483	1278	86.2	0	0	
88	4909	4338	88.4	6951	6196	89.1	175	162	92.6			
89	4835	4313	89.2	8046	7273	90.4	312	286	91.7			
90	5022	4496	89.5	8397	7654	91.2	341	304	89.1			
91	5617	5079	90.4	8177	7508	91.8	559	521	93.2			
92	6228	5688	91.3	8401	7758	92.3	364	335	92.0			
93	7160	6682	93.3	8677	8034	92.6	191	178	93.2			
94	8383	7900	94.2	8887	8297	93.4	379	358	94.5			
95	10 296	9784	95.0	8022	7573	94.4	373	348	93.3			
96	13 136	12569	95.7	7677	7350	95.7	389	352	90.5			
97	18 040	17431	96.6	7382	7122	96.5	0	0				
98	24 873	23835	95.8	4649	4484	96.5						
99	0	0		0	0							

<sup>a</sup>data not shared with XDQSO BOSS<sup>b</sup>data not shared with NBCKDE



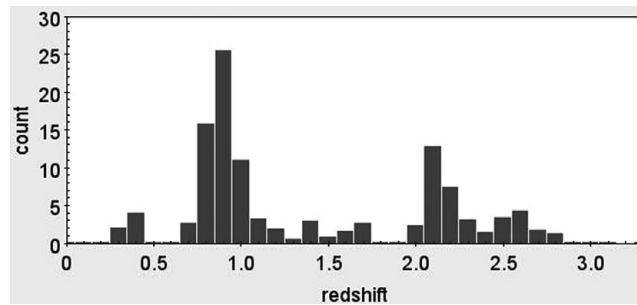


**Figure B1.** Count of spectroscopically confirmed redshifts for the colours  $ug = 0.2$   $gr = 0.2$   $ri = -0.1$   $iz = 0.4$ , binned by  $0.1 z$ .

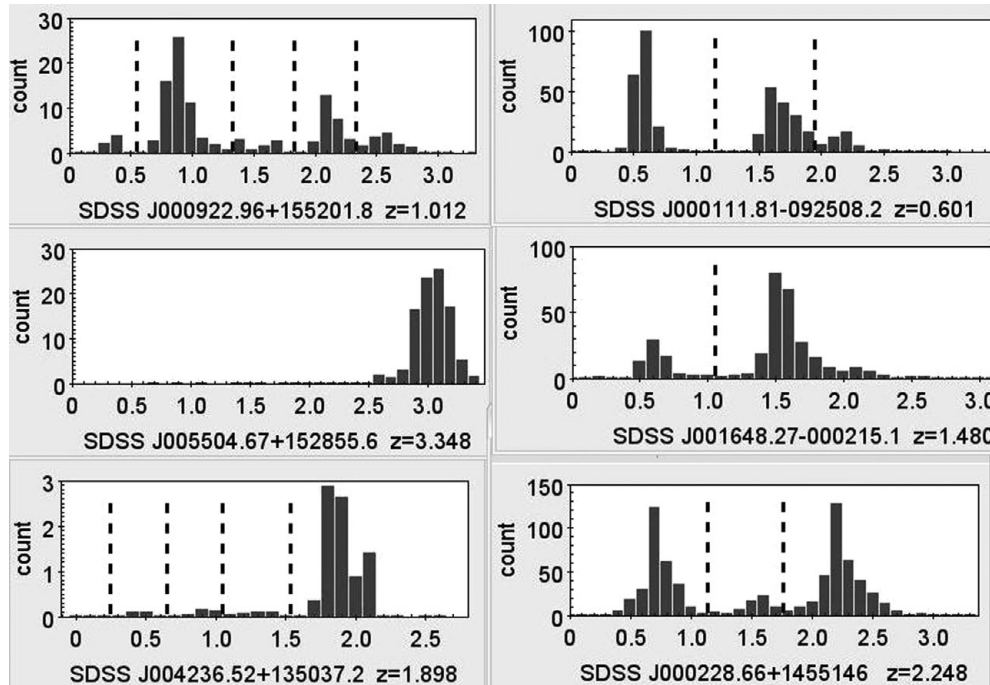


**Figure B2.** Six redshift profiles for photometric redshift calculations.

Figure B2 lower right has colours  $ug = 0.4$   $gr = 0.1$   $ri = 0.1$   $iz = 0.1$  and shows three clusters of which the left and right clusters are similar in size; summations show that the three clusters hold 41%, 8%, and 51%, respectively. My photometric redshift is 2.2, NBCKDE has 2.215, spectral is 2.248. This redshift profile came close to yielding no result as happens when the leading contenders are too closely matched; about 2.5% of objects get no photometric redshift because of this.

A comprehensive comparison of the photometric redshifts from this algorithm (based on the DR9 training set) compared with NBCKDE is available for inspection<sup>10</sup>. It lists 22 919 SDSS-DR10

quasars as the test data; these quasars were first presented in DR10 so there is no overlap with the training set. Accordingly, the true spectral SDSS-DR10 redshifts are also displayed, and the testing criterion is to treat each photometric redshift as a ‘hit’ if within  $0.5 z$  of the true spectral redshift. There it is seen that the NBCKDE hit rate is  $16\,658/22\,919 = 72.7\%$ , and the rainflow hit rate is  $16\,986/22\,919 = 74.1\%$ . No doubt the NBCKDE method is better than my own simple algorithm, but I had the advantage of the very large SDSS-DR9 training set. This good performance validates the assignment of these photometric redshifts to the XDQSO-only objects.

<sup>10</sup>at <http://quasars.org/docs/NBCKDE-MQ-redshifts.txt>